

Detection of MAPK activation to evaluate the efficacy and potency of KRAS/SOS1 inhibitors by AlphaLISA and HTRF technologies.

Key features

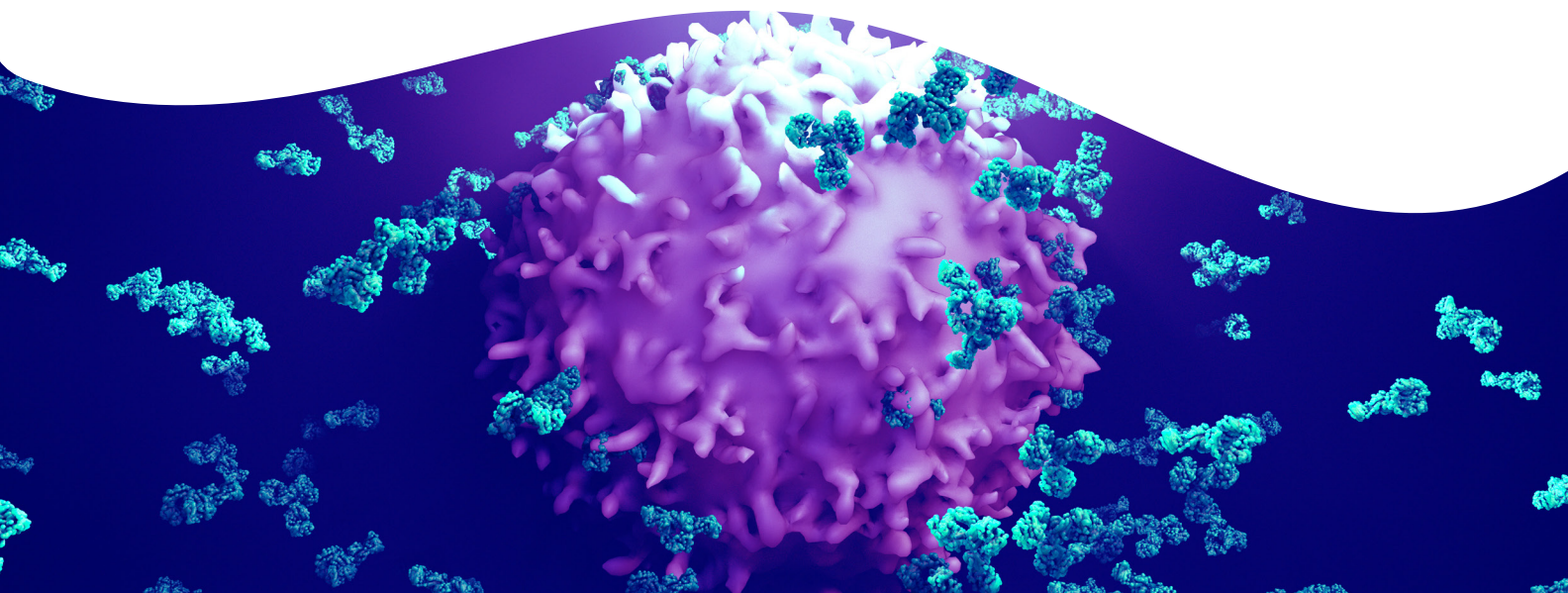
- Determine the effects of KRAS and SOS1 inhibitors in different human cancer cell lines
- Discriminate the cellular action of KRAS-targeting compounds and evaluate their effectiveness in modulating KRAS downstream pathways

Introduction

KRAS is a small GTPase implicated in various biological processes, such as cell proliferation, cell survival, and cell metabolism. The mutation of this proto-oncogene is well known to induce an uncontrolled proliferation and cell metabolism modifications in many cancer subtypes. It thereby contributes to the Warburg effect in cancer cells. Like the majority of small GTPases, KRAS binds to GDP in its inactive form or binds to GTP to switch into the active form. KRAS^{G12C} is one of the most commonly represented mutant forms in cancer, and leads to a permanently active state of KRAS¹. The Ras guanine nucleotide exchange factor, also called SOS1, is a GEF protein promoting the active form of KRAS. Upregulation of the KRAS / SOS1 interaction leads to cancer phenotypes.

Identifying new KRAS / GTP competitors and KRAS/SOS1 inhibitors is therefore a relevant strategy to control the biological processes involved in cancer growth by reducing KRAS activity, as well as the associated pathways². It is well known that KRAS induces activation of Mitogen-Activated Protein Kinase (MAPK), thus playing a central role in human cancers³.

The efficiency of the AlphaLISA[®] and HTRF[®] KRAS portfolios in identifying and classifying chemical compounds such as KRAS GTP competitors or KRAS/SOS1 inhibitors has been proven in a biochemical context. This application note provides a convincing demonstration of the reliability of the AlphaLISA and HTRF MAPK portfolios for the evaluation of the *in vitro* therapeutic profile of compounds in a cellular context.



Materials and methods

Reagents and consumables

- K-562 cells (ATCC, #CCL-243)
- Calu-1 cells (ATCC, #HTB-54)
- HT-29 cells (ATCC, #HTB-38)
- IDMD medium (ThermoFisher, #12440053)
- McCoy's 5A modified medium (ThermoFisher, #16600082)
- Fetal bovine serum (FBS), heat inactivated (ThermoFisher, #10082147)
- Penicillin-Streptomycin (ThermoFisher, #15140122)
- Epidermal Growth Factor Human (EGF) (Sigma-Aldrich, #E9644)
- Insulin-like Growth Factor-1 Human (IGF-1) (Sigma-Aldrich, #I3769)
- Proxiplate-384 plus, shallow well (Revvity, #6008280)
- AlphaPlate-384, light gray (Revvity, #6005350)
- HTRF total-ERK1/2 kit (Revvity, #64NRKPEG)
- HTRF Advanced phospho-ERK1/2 (Thr202/Tyr204) kit (Revvity, #64AERPEG)
- HTRF total-MEK1 kit (Revvity, #64NE1PEG)
- HTRF phospho-MEK1 (Ser218/222) kit (Revvity, #64ME1PEG)
- AlphaLISA® SureFire® Ultra™ Total ERK 1/2 Assay Kit (Revvity, #ALSU-TERK)
- AlphaLISA SureFire Ultra p-ERK1/2 (Thr202/Tyr204) Assay Kit (Revvity, #ALSU-PERK)
- AlphaLISA SureFire Ultra Total MEK1 Assay Kit (Revvity, #ALSU-TMEK1)
- AlphaLISA SureFire Ultra p-MEK1 (Ser218/222) Assay Kit (Revvity, #ALSU-PMEK1)

Principle of HTRF assays

HTRF® is a TR-FRET based technology, and stands for homogeneous time resolved fluorescence. It is based on the Fluorescent Resonance Energy Transfer (FRET) between two fluorophores, a donor and an acceptor. These fluorophores can be coupled to analyte-targeting antibodies in such a way that once bound, they come into proximity with one another. Excitation of the donor by an energy source (e.g. a flash lamp

or a laser) triggers an energy transfer towards the nearby acceptor, which in turn emits specific fluorescence at a given wavelength (Figure 1). The Total-protein assays or Phospho-protein assays quantify the expression level of total proteins or phosphorylated proteins in a cell lysate. Unlike Western Blot, the assay is entirely plate-based and does not require gels, electrophoresis, or transfer. The assays use two labeled antibodies: one coupled to a donor fluorophore, the other to an acceptor. Both antibodies are highly specific for a distinct epitope on the protein. In presence of the specific protein in a cell extract, the addition of these conjugates brings the donor fluorophore into close proximity with the acceptor and thereby generates a FRET signal. Its intensity is directly proportional to the concentration of the protein present in the sample, and provides a means of assessing the protein's expression under a no-wash assay format (Figure 1).

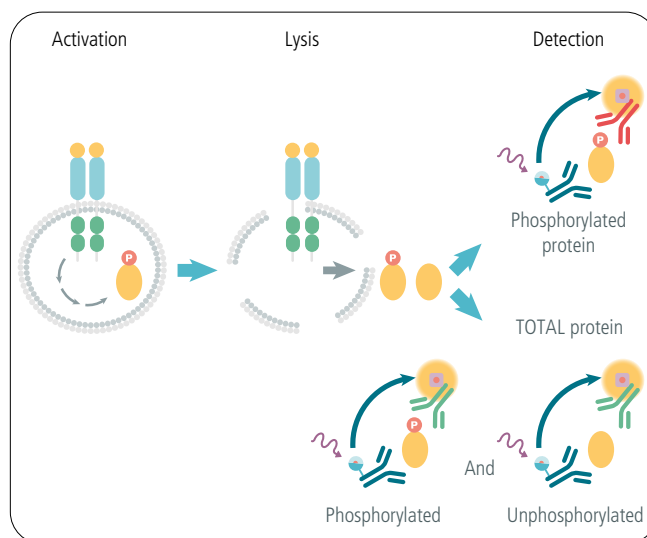


Figure 1: Principle of the Phospho/Total protein HTRF assays.

Principle of AlphaLISA SureFire Ultra assays

AlphaLISA® is a bead-based immunoassay technology used to study biomolecular interactions in a microplate format. The acronym "Alpha" stands for amplified luminescent proximity homogeneous assay. Some of the key features are that it is a non-radioactive, no-wash, homogeneous proximity assay. Binding of molecules captured on the beads and excitation of the donor lead to an energy transfer from the donor bead to the acceptor bead, ultimately producing a luminescent/fluorescent signal. In the AlphaLISA® SureFire® Ultra™ assay, donor beads are coated with streptavidin to capture one of the antibodies, which is biotinylated. Acceptor beads are coated with a proprietary CaptSure™ agent that immobilizes the other antibody, labeled with a CaptSure™ tag. In the presence of phosphorylated protein

or total protein, the two antibodies bring the donor and acceptor beads close together, generating a signal. The amount of light emission is directly proportional to the amount of phosphoprotein present in the sample (Figure 2).

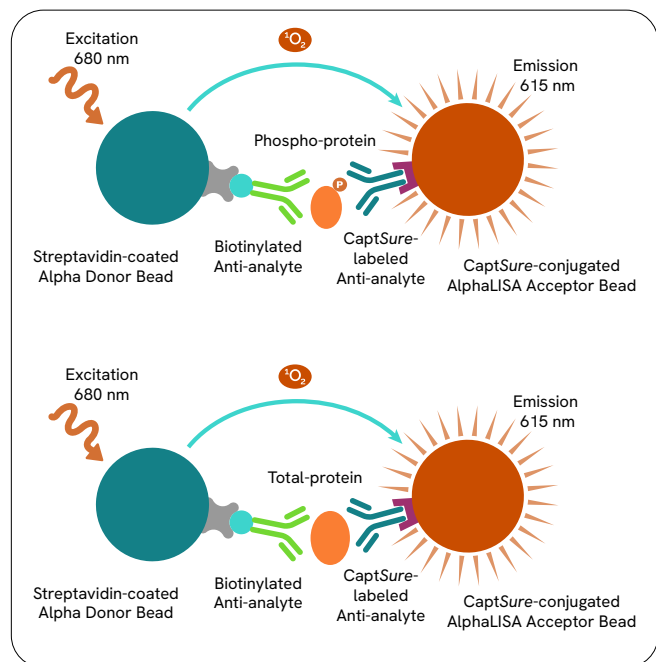


Figure 2: Principle of the Phospho/Total protein AlphaLISA SureFire Ultra assays.

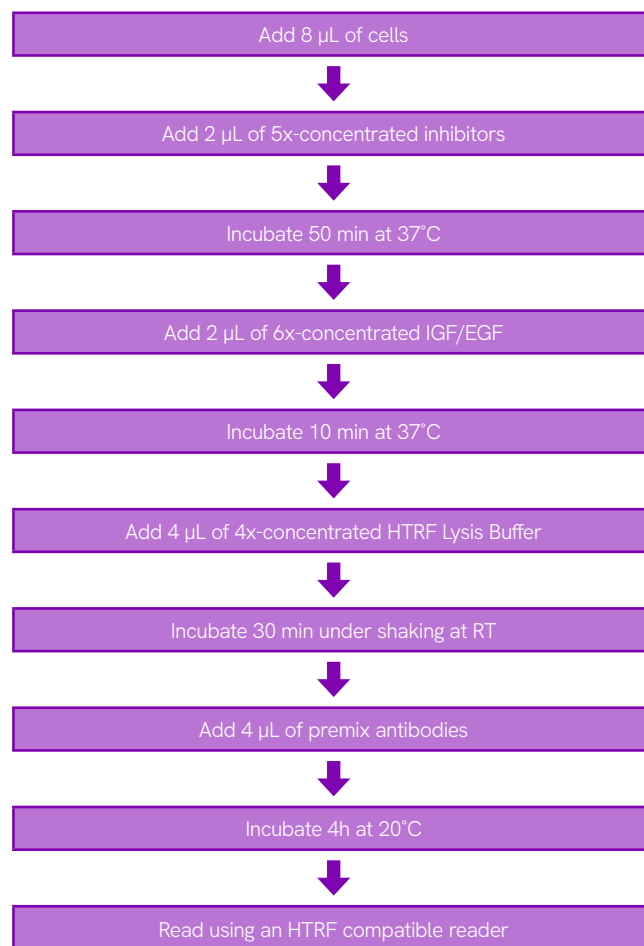
Cell cultures

K-562 cells (ATCC CCL-243) were grown at 37°C in Dulbecco's modified Eagle's medium (DMEM) culture medium, supplemented with 10% fetal bovine serum, 0.1% penicillin/streptomycin. Calu-1 cells (ATCC HTB-54) and HT-29 cells (ATCC HTB-38) were grown at 37°C in McCoy's 5a Medium Modified culture medium, supplemented with 10% fetal bovine serum, 0.1% penicillin/streptomycin.

HTRF protocol

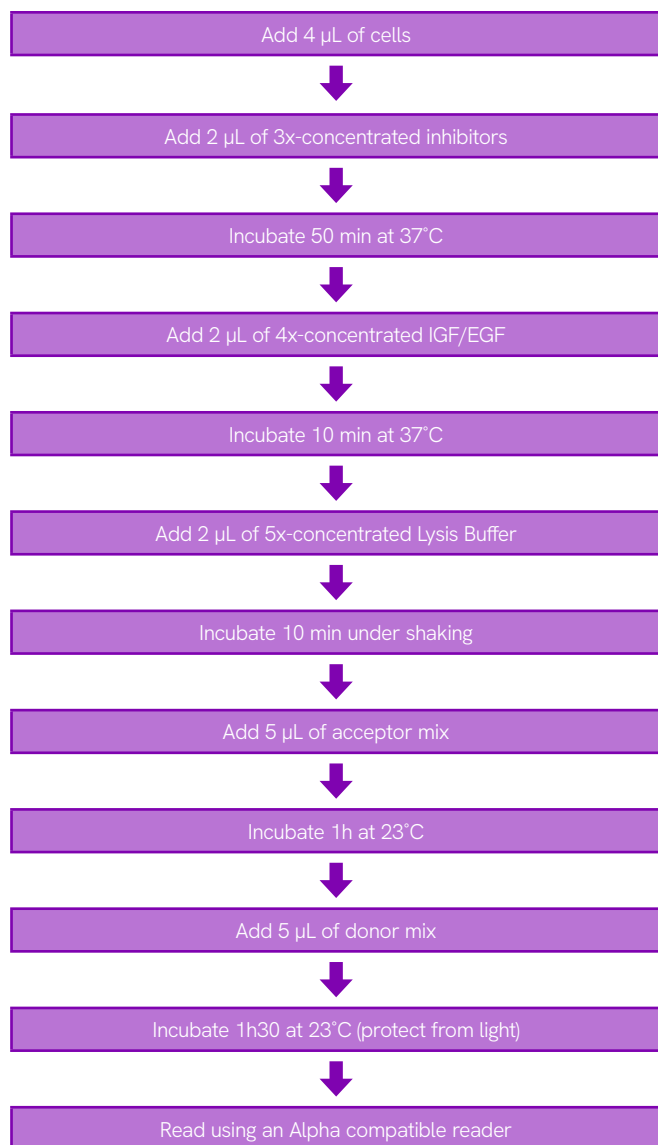
The HTRF assays were carried out using the standard 1-plate protocol for each kit. Briefly, whole cells were plated in a small volume white detection plate (Proxiplate-384 wells) at the appropriate cell density (40 000 cells/well and 60 000 cells/well for respectively the K-562 cells and the Calu-1 cells). 2 µL of a 5x-concentrated inhibitor (range of 10⁻¹¹ to 10⁻⁴ M) were added to the cells, and incubated for 50 min at 37°C. Then 2 µL of a 6x-concentrated premix IGF/EGF at 600 nM were added to induce the phosphorylation of the MAPK pathway, and the samples were incubated for 10 min at 37°C. Cells were next incubated for 30 min at room temperature under shaking with 4 µL of the appropriate supplemented lysis buffer (4X). A premix of

antibody solution was then prepared, and 4 µL were added. The plate was incubated at 20°C for 4h. Lastly, the plate was read on an HTRF Technology-compatible plate reader.



AlphaLISA protocol

The AlphaLISA assays were carried out using the standard 1-plate protocol for each kit. Briefly, whole cells were plated in a small volume white detection plate (SV AlphaPlate-384 wells) at the appropriate cell density (30 000 cells/well and 60 000 cells/well for respectively the HT-29 cells and the Calu-1 cells). 2 µL of a 3x-concentrated inhibitor (range of 10⁻¹¹ to 10⁻⁴ M) were added to the cells, and incubated for 50 min at 37°C. Then 2 µL of a 4x-concentrated premix IGF/EGF at 400 nM were added to induce the phosphorylation of the MAPK pathway, and incubated for 10 min at 37°C. Cells were next incubated for 30 min at room temperature under shaking with 2 µL of the appropriate supplemented lysis buffer (5X). The acceptor beads were then added, and incubated for 1h at 23°C. The donor beads were added, and the samples were incubated for 1h at 23°C under subdued lighting. The plate was read on an Alpha Technology-compatible plate reader.



Data analysis

The AlphaLISA signal was measured on an Alpha compatible plate reader using default values for Alpha detection of the fluorescence label. Data was analyzed in GraphPad Prism (version 9; GraphPad Software Inc.) using non-linear 3 parameter logistic regression for the dose-response curves. The HTRF signal was measured on an HTRF compatible plate reader using HTRF settings. Excitation with a laser followed, and emissions at 620 nm (donor reference signal) and 665 nm (acceptor signal) were recorded. Data is reported as the HTRF ratio of acceptor to donor signal = $(665/620) \times 10,000$. For normalization, the data were normalized to vehicle (= 100%). The results were analyzed in GraphPad Prism using non-linear 3 parameter logistic regression for the dose-response curves.

Results

Comparison of phospho-ERK modulation by the SOS1/KRAS inhibitor BAY-293 on two cellular models

p-ERK1/2 (Thr202/Tyr204) and t-ERK1/2 HTRF assays were performed to quantify the phosphorylated form of ERK1/2 or the total form of ERK1/2 from K-562 cells and Calu-1 cells stimulated with 100 nM concentration of hEGF and hIGF-1. A dose-response curve with BAY-293, a SOS1/KRAS interaction inhibitor, was prepared with the two cell lines (Figure 3). The results obtained with human leukemia K-562 cells expressing the KRAS^{WT} form showed a total inhibition of ERK1/2 phosphorylation with an IC₅₀ of 61 nM (Figure 3A). No modulation of the total level of ERK1/2 was observed (Figure 3B). These results were consistent with the literature. Previously, Hillig R. et al showed a potency of BAY-293 at 180 nM in this human leukemia cell line⁴.

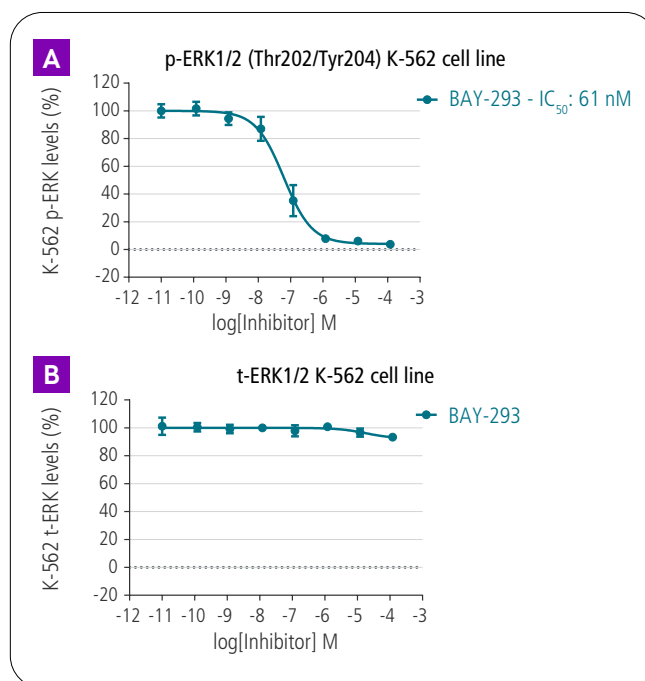


Figure 3: Detection of phosphorylated ERK1/2 proteins and total ERK1/2 proteins by HTRF in the K-562 wild-type KRAS cell line. A) p-ERK1/2 levels. B) t-ERK1/2 levels.

In parallel, the results obtained with human lung cancer Calu-1 cells expressing the KRAS^{G12C} form showed a partial inhibition of ERK1/2 phosphorylation, with an IC₅₀ of 2100 nM (Figure 4).

BAY-293 seems to be more potent in the leukemia cell line than in the human lung cancer cell line. Interestingly, BAY-293 induced an inhibition of ERK1/2 phosphorylation of about 60% in this KRAS mutated cell line compared to the K-562 cell line (Figure 4A). BAY-293 efficacy seems to be dependant on the cancer cell line. No modulation of the total level of ERK1/2 was observed (Figure 4B). These results were consistent with the literature. Hillig showed a potency of BAY-293 around 700 nM in the Calu-1 cell line, and a partial inhibition of phosphorylation at around 50%⁴.

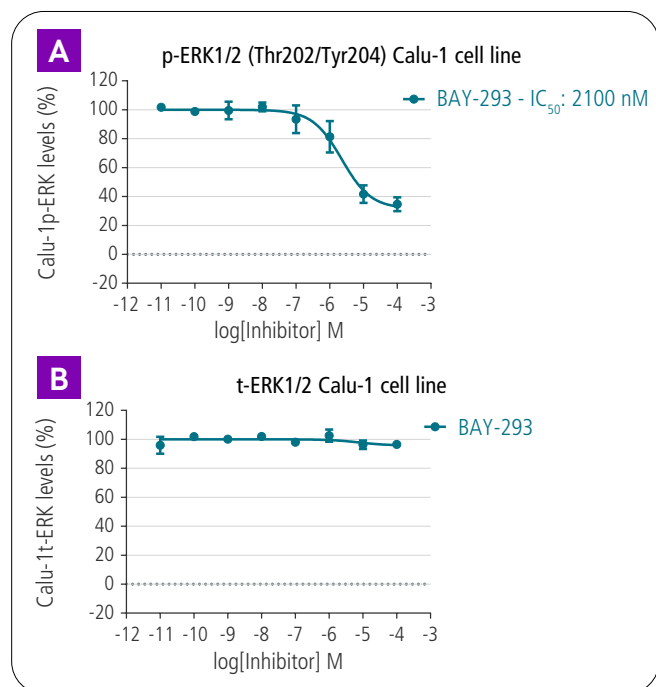


Figure 4: Detection of phosphorylated ERK1/2 proteins and total ERK1/2 proteins by HTRF in the Calu-1 KRAS^{G12C} cell line. A) p-ERK1/2 levels. B) t-ERK1/2 levels.

The p-ERK1/2 (Thr202/Tyr204) and t-ERK1/2 HTRF kits have enabled a demonstration of the efficacy and potency of an inhibitor in various human cancer cell lines. These results illustrate the importance of screening compounds in various cellular models to determine the cellular action of inhibitors. The HTRF kits enable the rapid, sensitive, and quantitative detection of phospho- and total-proteins from various cell lines.

Demonstration of the potency and efficacy of an SOS1 inhibitor and the selectivity of a KRAS^{G12C} inhibitor on a KRAS^{G12C} cell line

p-ERK1/2 (Thr202/Tyr204) and t-ERK1/2 AlphaLISA *SureFire Ultra* assays were performed to quantify the phosphorylated form of ERK1/2 or the total form of ERK1/2 from Calu-1 cells stimulated with 100 nM concentration of hEGF and hIGF-1. Dose-response curves were prepared with BAY-293, a SOS1/KRAS interaction inhibitor, and AMG-510, a selective KRAS^{G12C} inhibitor⁵ (Figure 5). The results obtained with human lung cancer Calu-1 cells expressing the KRAS^{G12C} form showed that AMG-510 was more potent and efficient in inhibiting the phosphorylation of ERK1/2 than BAY-293 (Figure 5A). The IC₅₀ were respectively 337 nM and 972 nM. As expected, no modulation of the total level of ERK1/2 was observed (Figure 5B).

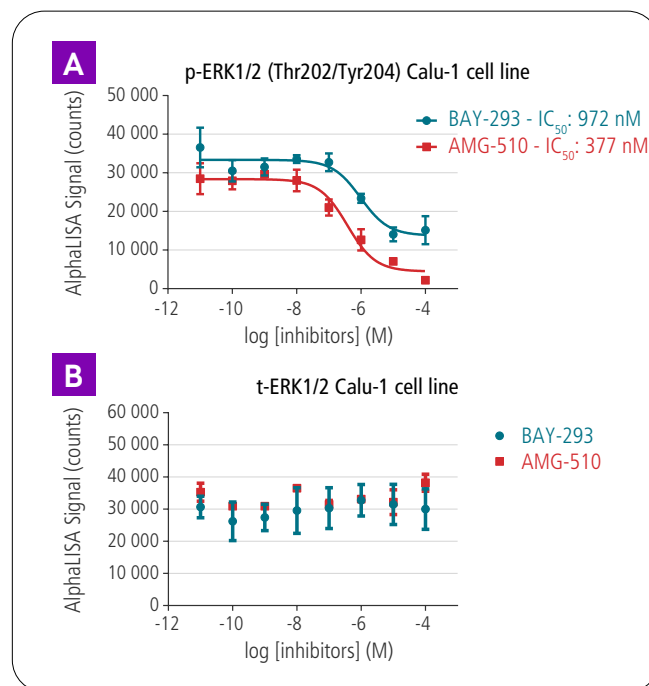


Figure 5: Detection of phosphorylated ERK1/2 proteins and total ERK1/2 proteins by AlphaLISA in the Calu-1 KRAS^{G12C} cell line. A) p-ERK1/2 levels. B) t-ERK1/2 levels.

The p-MEK1 (Ser218/222) AlphaLISA *SureFire Ultra* assay was performed to quantify the phosphorylated form of MEK1 from Calu-1 cells stimulated with 100 nM concentration of hEGF and hIGF-1. The results obtained with this assay were correlated with the previous results obtained using the p-ERK1/2 (Thr202/Tyr204) AlphaLISA *SureFire Ultra* assay. As illustrated by these results, AMG-510 was more potent and efficient in inhibiting the phosphorylation

of MEK1 than BAY-293 (Figure 6). The IC_{50} of AMG-510 was 127 nM, while that of BAY-293 was 737 nM. No modulation of the total level of MEK1 was observed (data not shown).

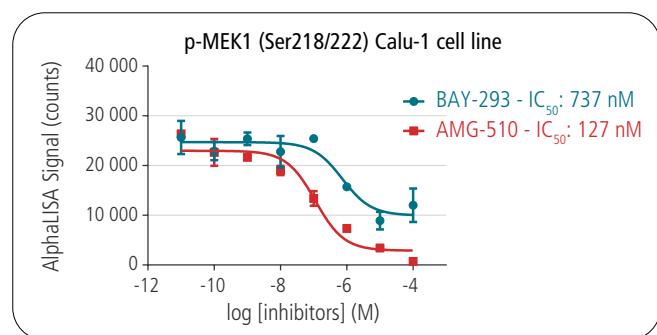


Figure 6: Detection of phosphorylated MEK1 by AlphaLISA in the Calu-1 KRAS^{G12C} cell line.

The p-ERK1/2 (Thr202/Tyr204) and p-MEK1 (Ser218/222) AlphaLISA *SureFire Ultra* kits have highlighted the efficacy and potency of an SOS1 inhibitor and a KRAS^{G12C} inhibitor in reducing MAPK activation. These two compounds show promising potential for the reduction of the proliferative effect promoted by the MAPK pathway.

Demonstration of the potency and efficacy of an SOS1 inhibitor and the selectivity of a KRAS^{G12C} inhibitor on a KRAS^{WT} cell line

p-ERK1/2 (Thr202/Tyr204) AlphaLISA *SureFire Ultra* assays were performed to quantify the phosphorylated form of ERK1/2 from HT-29 cells stimulated with 100 nM concentration of hEGF and hIGF-1. Dose-response curves were prepared with BI-3406, an SOS1/KRAS interaction inhibitor, and AMG-510, a selective KRAS^{G12C} inhibitor (Figure 7). As expected, the results obtained with human colorectal cancer HT-29 cells expressing the KRAS^{WT} form showed that AMG-510 had no effect on the phosphorylation of ERK1/2 on this cell line. In fact, AMG-510 was a selective KRAS^{G12C} inhibitor. On the other hand, BI-3406 showed a partial inhibition of ERK1/2 phosphorylation, with an IC_{50} of 128 nM. These results were consistent with the literature. Hofmann, M. et al. profiled BI-3406 in a larger panel of cancer cell lines to evaluate its capacity to reduce cell proliferation⁶. The study demonstrated that BI-3406 sensitivity was correlated with the KRAS forms.

BI-3406 was less potent in inhibiting the proliferation of the colorectal cancer cell line HT-29, that expresses the KRAS wild-type form, than cells expressing KRAS mutated forms. No modulation of the total level of ERK1/2 was observed (data not shown).

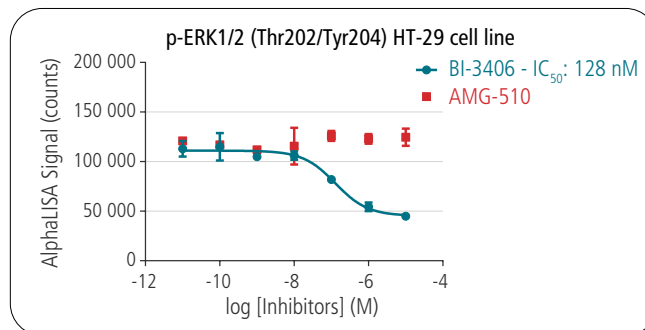


Figure 7: Detection of phosphorylated ERK1/2 proteins by AlphaLISA in the HT-29 wild-type KRAS cell line.

The p-MEK1 (Ser218/222) AlphaLISA *SureFire Ultra* assay was performed to quantify the phosphorylated form of MEK1 from Calu-1 cells stimulated with 100 nM concentration of hEGF and hIGF-1. The results obtained with this assay were correlated with the previous results obtained using the p-ERK1/2 (Thr202/Tyr204) AlphaLISA *SureFire Ultra* assay. As illustrated by these results, AMG-510 was more potent and efficient in inhibiting the phosphorylation of MEK1 than BAY-293 (Figure 6). The IC_{50} of AMG-510 was 127 nM, while that of BAY-293 was 737 nM. No modulation of the total level of MEK1 was observed (data not shown).

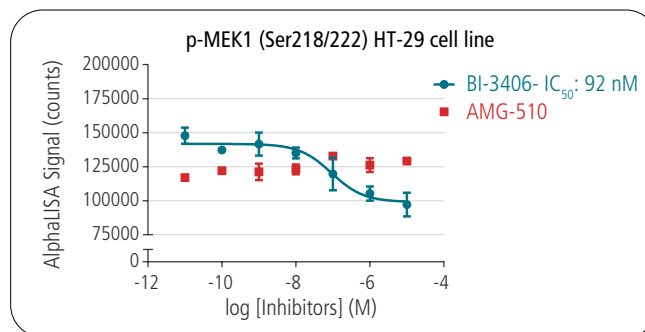


Figure 8: Detection of phosphorylated MEK1 by AlphaLISA in the HT-29 wild-type KRAS cell line.

Conclusion

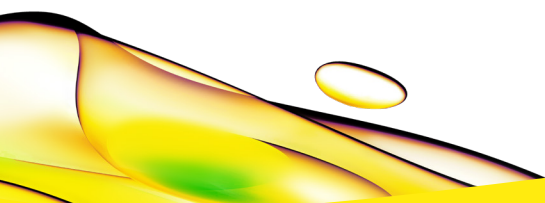
In this application note, we have demonstrated that it is possible to determine the effects of KRAS and SOS1 inhibitors in various human cancer cell lines. Our KRAS product portfolio of biochemical binding assays enables first screening of inhibitors to evaluate their ability to bind and inhibit KRAS/SOS1 interactions and/or KRAS/GTP active form induction. Furthermore, our MAPK portfolio of cellular signaling assays enables discrimination between the cellular action of the hit compounds highlighted in the first step, and evaluation of their efficacy in modulating the downstream pathways of KRAS. In conclusion, the homogeneous no wash AlphaLISA and HTRF p-MEK1(Ser218/222), t-MEK1, p-ERK1/2(Thr202/Tyr204), and t-ERK1/2 kits are efficient tools for the estimation of a therapeutic profile for KRAS-targeting compounds in various cancer cell lines.

Author

Emilie Eiselt

References

1. Liu, P. et al. Targeting the untargetable KRAS in cancer therapy. *Acta Pharm. Sin. B.* 2019 Sep;9(5):871-879. PMID : 31649840
2. Kessler, D. et al. Druggable and undruggable pocket on KRAS. *PNAS.* 2019, 32, 15823-15829. PMID : 31332011
3. Drosten, M. et al. Targeting the MAPK Pathway in KRAS-Driven Tumors. *Cancer Cell.* 2020 Apr 13; 37(4):543-550. PMID: 32289276
4. Hillig, R. et al. Discovery of potent SOS1 inhibitors that block RAS activation via disruption of the RAS-SOS1 interaction. *PNAS.* 2019 Feb 12; 116(7):2551-2560. PMID: 30683722
5. Lanman, B. et al. Discovery of a Covalent Inhibitor of KRASG12C (AMG 510) for the Treatment of Solid Tumors. *J Med. Chem.* 2020 Jan 9;63(1):52-65. PMID: 31820981
6. Hofmann, M. et al. BI-3406, a Potent and Selective SOS1-KRAS Interaction Inhibitor, is effective in KRAS-Driven Cancers through Combined MEK Inhibition. *Cancer Discov.* 2020 Aug 19; 10.1158/2159-8290. PMID: 32816843



revvity